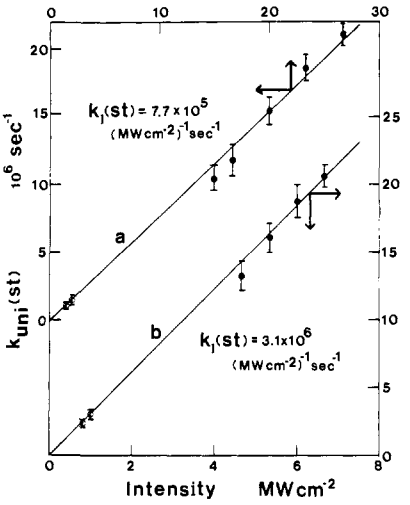


**Figure 16.** Plot of $k_{uni}(st)$ vs. intensity for cross-section models a and b: O, 2-$\mu$s pulse; 300-ns pulse. The $k_{uni}(st)$ values were calculated from the linear portion of the curves in Figure 14. The slope of this plot provides $k_1(st)$, where $k_1(st) = k_{uni}(st)/I$.

where $t_p$ is the laser pulse length. Therefore, the steady-state region defined with respect to time can be converted to $F_R$ vs. $\phi$ which are experimentally more useful. The steady-state region is also reached only for $F_R > 80\%$ in the ln $(1 - F_R)$ vs. $\phi$ plot (see Figure 15). Since $F_R > 80\%$, the postpulse contribution to the overall reaction yield is therefore small and in the steady-state or high-fluence region $F_R$ can be directly related to the experimental reaction yield in a bulb experiment.

The biparticular rate constants,[10] $k_I(st) = k_{uni}(st)/I$, obtained from the linear part of the ln $(1 - F_R)$ vs. $\phi$ plots are $(0.72 \pm 0.07) \times 10^6$ and $(2.8 \pm 0.3) \times 10^6$ $(MW/cm^2)^{-1}$ $s^{-1}$ for models a and b, respectively. These results may be compared with the values $0.77 \pm 0.03 \times 10^6$ and $3.1 \pm 0.3 \times 10^6$ $(MW/cm^2)^{-1}$ $s^{-1}$ for model a and b, respectively, obtained from Figure 16. The good agreement demonstrates that numerical accuracy is retained for the high fractional reaction necessary to reach steady state. The $k_I(st)$ values do not seem to depend on the intensity. This is very important because experimental plots of ln $(1 - F_R)$ vs. $\phi$ can be made with data for which time (pulse length) was held constant but intensity varied in order to change fluence. The serious problem of extracting experimental $k_1(st)$ values is the need to accurately measure $F_R$ at very high fractional reaction; the present calculations suggest the limiting slope should be derived from data for which $P(\phi) \geq 0.80$. However, on the positive side, $k_I(st)$ is sensitive to the cross-section model. Thus, $k_I(st)$ is an important experimental measurement.

**Acknowledgment.** This work was supported by the National Science Foundation under Grant 77-21380 and also in part by Grant 77-22645. We thank Professor Kenneth G. Kay for reading the manuscript and for constructive criticism.

# Indirect Detection of $^{199}$Hg NMR: Adducts of Ethylmercury Phosphate with Amino Acids and Ribonuclease

**D. A. Vidusek, M. F. Roberts,* and Geoffrey Bodenhausen**

*Contribution from the Chemistry Department and the Francis Bitter National Magnet Laboratory, Massachusetts Institute of Technology, Cambridge, Massachusetts 02139.*
*Received December 14, 1981*

**Abstract:** $^{199}$Hg NMR spectroscopy is used to examine the interaction of the toxic organomercurial ethylmercury phosphate with various amino acids. Because of the relative insensitivity of $^{199}$Hg and the low concentrations of biological molecules, a heteronuclear spin-echo and a two-dimensional technique involving a double transfer of polarization are used to bypass the concentration limits of direct detection. The chemical shifts of $^{199}$Hg cover a wide range (600 ppm for ethylmercury derivatives) and are diagnostic for the identity of the ethylmercury adduct. Using the mercury chemical shifts and pH stability determined for adducts of the ethylmercuric ion with individual amino acids, we suggest that the ethylmercury–ribonuclease adduct involves modification of the N-terminal lysine residue.

Recent interest in organomercurials is based on their extreme toxicity.[1] Within a cell these compounds may react with proteins, nucleic acids, and even membranes (amino phospholipids). Complexes of organomercurials, typically methylmercury, with the individual components of these macromolecular assemblies have been studied in some detail. While cysteine forms nearly covalent complexes with methylmercury (this is often exploited in forming heavy atom derivatives of proteins with free sulfhydryl groups),[2] nitrogen-bound complexes (histidine, tryptophan, free amine groups) and much weaker carboxylate complexes can also form.[3] Methylmercury binds to N-3 of uridine and cytidine and to the same site in purine nucleosides and nucleotides.[4] Changes in the sedimentation characteristics of DNA show that methylmercury reacts with the imino (NH) bonds of thymine and guanine[5] as well. More complex model systems, with several different reactive species, have not been examined because most analytical techniques are not selective or sensitive enough to identify the mercury ligand.

(1) (a) Curley, A.; Sedlak, V.; Girling, E.; Hawk, R.; Barthel, W.; Pierce, P.; Likosky, W. *Science* (Washington, D.C.) **1971** *172*, 65. (b) Bache, C.; Gutenmann, W.; Lisk, D. *Ibid.* **1971**, *172*, 951. (c) Fridberg, L.; Vostel, J. "Mercury in the Environment; An Epidemiological and Toxicological Appraisal"; CRC Press: Cleveland, OH, 1972.

(2) (a) Banner, D. W.; Bloomer, A. C.; Petsko, G. A.; Phillips, D. C.; Pogson, C. I.; Wilson, I. A. *Nature* (*London*) **1975**, *255*, 609. (b) Tsernoglou, D.; Petsko, G. A. *FEBS Lett.* **1976**, *68*, 1.

(3) (a) Simpson, R. *J. Am. Chem. Soc.* **1961**, *83*, 4711. (b) Simpson, R. *Ibid.* **1964**, *86*, 2059. (c) Libich, S.; Rabenstein, D. *Anal. Chem.* **1973**, *45*, 118. (d) Rabenstein, D.; Ozubko, R.; Libich, S.; Evans, C.; Fairhurst, M.; Suvanprakorn, C. *J. Coord. Chem.* **1974**, *3*, 263.

(4) (a) Mansy, S.; Wood, T.; Sprowles, J.; Tobias, R. *J. Am. Chem. Soc.* **1974**, *96*, 1761. (b) Mansy, S.; Tobias, R. *Ibid.* **1974**, *96*, 6874.

(5) (a) Gruenwedel, D.; Davidson, N. *Biopolymers* **1967**, *5*, 847. (b) Gruenwedel, D. *Eur. J. Biochem.* **1972**, *25*, 544.

0002-7863/82/1504-5452$01.25/0 

$^{199}$Hg NMR spectroscopy is in principle an excellent probe of organomercury adducts.[6] $^{199}$Hg ($I = {}^1/_2$) has a chemical shift range of 2500 ppm,[7] and the few published INDOR[8] and Fourier transform[9a,b] studies suggest that the chemical shift can be correlated with the mercury ligands. But the inherent insensitivity of $^{199}$Hg (16.9% natural abundance, 0.6% as sensitive as an equal number of protons) makes studying biological materials difficult. With conventional NMR direct detection techniques, including large (15–10 mm) sample tubes and long accumulation times, concentrations exceeding the solubility limits of most proteins and nucleic acids would be necessary to obtain $^{199}$Hg NMR spectra.[10]

A variety of indirect detection techniques have been devised to improve the observation of insensitive nuclei. We have used two such techniques to measure the $^{199}$Hg chemical shift of ethylmercury phosphate[11] as a function of pH and added ligand. A spin-echo[12] sequence with strong rf pulses to cover a broad spectral window around the $^{199}$Hg Larmor frequency determines the $^{199}$Hg chemical shift to ±12 ppm. In this fashion, concentrations of mercurials as low as 4 mM (400–500 μL in 5-mm tubes) can be examined in a relatively short amount of time. For more precise chemical shifts (±5 Hz), a two-dimensional technique[13] involving a double transfer of polarization (enhanced heteronuclear spectroscopy)[14] can be used. For $CH_3CH_2HgX$ adducts with amino acids and *N*-acetyl derivatives, X can be easily identified as oxygen, nitrogen, or sulfur from the $^{199}$Hg chemical shift determined with the spin-echo technique. Hg–N adducts can be further differentiated by more precise chemical shift information (2-D technique) and pH stability. These data are then used to identify lysine as the probable residue in ribonuclease A that reacts with ethylmercury phosphate.

## Experimental Section

**Sample Preparation.** Ethylmercury phosphate (Chem Service), *p*-(hydroxymercuri)benzoate (Sigma), and amino acids and *N*-acetyl derivatives (Sigma) were used as received. Bovine pancreatic ribonuclease A was obtained from Worthington. Stock solutions of each component in 99.7% $D_2O$ (Merck Isotopes) were mixed to form the adducts. Mixtures (usually 40 mM of each component for amino acid derivatives; 4 mM equimolar ribonuclease and ethylmercury phosphate) were lyophilized and reconstituted with 99.96% $D_2O$ (Aldrich) to minimize the HDO resonance. The apparent pH was adjusted to the desired value with NaOD and $DNO_3$. The introduction of chloride ions was carefully avoided to prevent formation of insoluble ethylmercury chloride.

Ribonuclease activity was assayed by a modification of the procedure of Murdock et al.[15] Measurements were made on a Perkin-Elmer Lambda 3 spectrophotometer.

**$^{199}$Hg NMR Detection.** NMR spectra were obtained on a Bruker 270 spectrometer equipped with a Nicolet 1080 data system. The spectrometer was modified as follows: the 5-mm probe, which was originally designed for fluorine-19, was retuned for proton pulsing and observation; the decoupling coil was retuned for the mercury-199 Larmor frequency (48.3 MHz). An external frequency synthesizer generated a signal at 48.3 MHz, which was gated, phase shifted with a double-balanced mixer, and amplified by a Boonton 230A power amplifier to a level of 9 W. Under these conditions the mercury 90° flip angle was determined to be 100 μs. The spectrometer itself was run in the normal proton mode. The pulse sequences were generated by modifying the computer program controlling the Nicolet 293 pulse programmer, allowing both the spectrometer and the external apparatus to generate pulses of the appropriate frequencies simultaneously.

Detection of the mercury resonances was achieved through two pulse techniques. The first of these, the classic spin-echo technique, was adapted to efficient heteronuclear use by applying a 180° pulse to the mercury-199 spin simultaneously with a 180° proton pulse. The pulse sequence and the corresponding magnetization vectors in the rotating frame are shown in Figure 1. The technique has been described previously.[6] The scalar coupling $^3J_{HHg}$ of the ethylmercury methyl protons (250–350 Hz) produces satellites in the proton spectrum that are well-separated from other resonances. Proton spectra are acquired while stepping through the $^{199}$Hg frequency range with pulses capable of covering 5-kHz increments. As noted in the magnetization vector diagrams, when the frequency of the mercury pulse matches the Larmor frequency of the mercury nucleus, inversion of the satellite occurs. Since the $^{199}$Hg chemical shift range is so large (2500 ppm; 121 kHz at this field strength), this technique allows rapid determination of the mercury chemical shift to ±500 Hz (12 ppm) by determining the frequency for maximum satellite inversion. For example, with 40 mM ethylmercury phosphate (400–500 μL) 12 scans are acquired for each trial $^{199}$Hg frequency. Including the time required for the fast Fourier transform algorithm, this amounts to about 16 s per spectrum. The entire ethylmercury chemical shift range (600 ppm; 30 kHz at this field) can be examined with 30 spectra in under 10 min. Direct detection of $^{199}$Hg generally requires 1.5 mL of 1.0 M sample in order to observe a spectrum within the same time period.

A more accurate measurement of the $^{199}$Hg chemical shift is achieved with a two-dimensional technique based on the transfer of polarization from protons to mercury and then back to protons. The pulse sequence

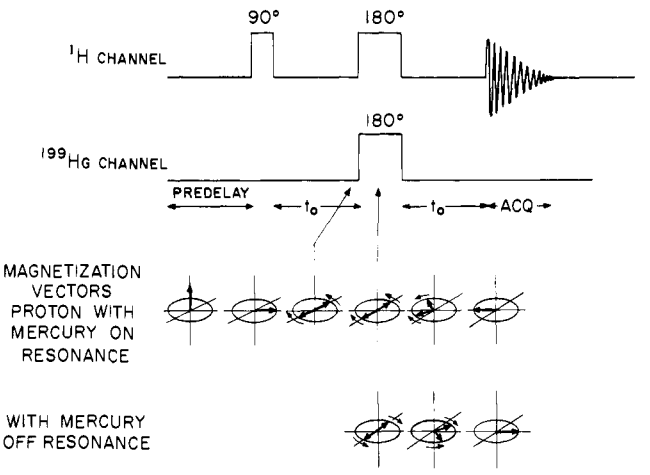


**Figure 1.** Pulse sequence for the heteronuclear spin-echo detection of $^{199}$Hg NMR. Protons undergo a $90°-t_0-180°-t_0$ sequence with $t_0 = (2\ {}^3J_{HHg})^{-1} = 1.52$ ms for EMP. A 180° pulse on the mercury channel (200 μs) is applied in synchronism with the $^1$H refocusing pulse. Vectors in the rotating frame illustrate the nuclear magnetization throughout the duration of the sequence. Note that the detector sees the scalar-coupled satellite as a negative signal with mercury irradiation on-resonance and a positive signal with off-resonance mercury irradiation.

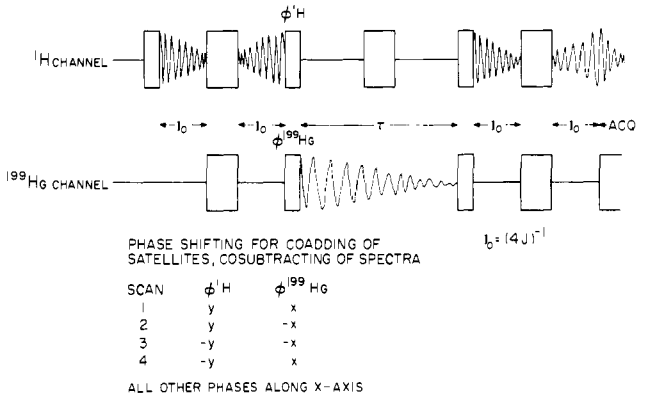


**Figure 2.** Pulse sequence for the two-dimensional heteronuclear spin-echo indirect detection experiment, used to obtain proton-decoupled $^{199}$Hg spectra. The delay, $t_0$, is equal here to $(4^3J_{HHg})^{-1} = 0.76$ ms for EMP. $\tau$ is determined by the desired sweep width along the mercury-199 chemical shift axis. Because of experimental limitations, $\tau_{min} = 0.001$ s, which corresponds to a sweep width of 2500 Hz (50 ppm for $^{199}$Hg at this field).

(6) Roberts, M. F.; Vidusek, D. A.; Bodenhausen, G. *FEBS Lett.* **1980**, *117*, 311.
(7) Sens, M. A.; Wilson, N. K.; Ellis, P. D.; Odom, J. D. *J. Magn. Reson.* **1975**, *19*, 323.
(8) Arnet, F. A. L.; Sudmeier, J. L. *J. Magn. Reson.* **1969**, *1*, 124.
(9) (a) Maciel, G. E.; Borzo, M. *J. Magn. Reson.* **1973**, *10*, 388. (b) Sudmeier, J.; Birge, R.; Perkins, T. *Ibid.* **1978**, *30*, 491.
(10) Sudmeier, J. L.; Perkins, T. G. *J. Am. Chem. Soc.* **1977**, *99*, 7732.
(11) The abbreviations used are: EMP, ethylmercury phosphate; pHMB, *p*-(hydroxymercuri)benzoate.
(12) (a) Hahn, E. *Phys. Rev.* **1950**, *80*, 580. (b) Emshwiller, M.; Hahn, E.; Kaplan, D. *Ibid.* **1960**, *118*, 414.
(13) Bodenhausen, G.; Ruben, D. J. *Chem. Phys. Lett.* **1980**, *69*, 185.
(14) Maudsley, A. A.; Ernst, R. R. *Chem. Phys. Lett.* **1977**, *50*, 368.
(15) Murdock, A.; Grist, K.; Hirs, C. *Arch. Biochem. Biophys.* **1966**, *114*, 375.

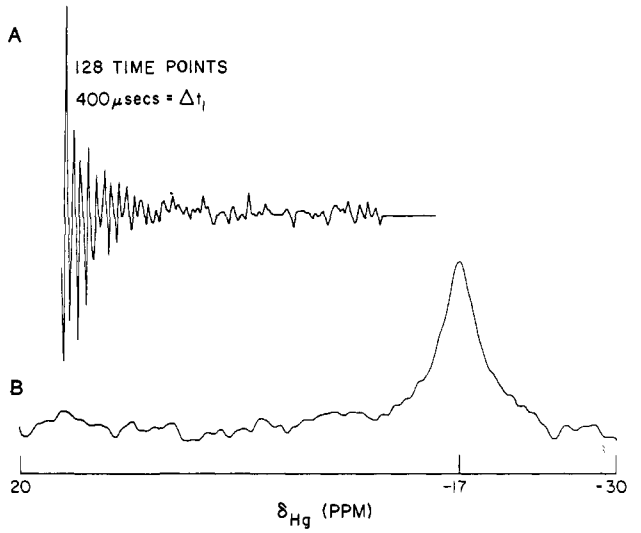


**Figure 3.** (A) Mercury-199 interferogram constructed by monitoring the amplitude of the scalar-coupled methyl satellite during the course of the heteronuclear two-dimensional experiment. The frequency spectrum shown (B) is obtained by Fourier transformation of the interferogram. The carrier frequency of the mercury pulse determines the frequency value of the spectrum endpoint.

is illustrated in Figure 2. The technique has been described in detail by Bodenhausen and Ruben[13] as applied to the indirect detection of nitrogen-15. With the external frequency synthesizer set close to the mercury resonance, the amplitude of the scalar-coupled satellite is monitored at time intervals $n\Delta t_1$, where $\Delta t_1$ is related to the size of the mercury window. The time course of this satellite modulation yields a $^{199}$Hg interferogram analogous to a free-induction decay (Figure 3A). A second Fourier transform (without quadrature) of this interferogram produces the proton-decoupled $^{199}$Hg spectrum (Figure 3B). The maximum theoretical sensitivity advantage of indirect detection is about 200-fold. Experimentally, less sensitivity is obtained, primarily due to spectral artifacts in the subtraction routine.

## Results and Discussion

**Ethylmercury Phosphate $^{199}$Hg Chemical Shifts.** The $^1$H NMR spectrum of ethylmercury phosphate in $D_2O$ shows distinct methyl and methylene regions. The methyl region consists of a major triplet ($^3J_{HH}$ = 8 Hz) flanked by two weak satellite triplets resulting from coupling of the methyl protons to $^{199}$Hg ($^3J_{HHg}$ = 250–350 Hz). The methylene region consists of a major quartet also flanked by mercury coupled satellites ($^2J_{HHg}$ = 175–275 Hz). There is no evidence of any $^{31}$P coupling to these protons. Furthermore, the $^1$H-noise-decoupled $^{31}$P NMR spectrum of ethylmercury phosphate shows a single narrow resonance. The lack of scalar coupling to the $^{199}$Hg suggests that the ethylmercury ion is "free" or hydrated in solution and shows no covalent interaction with the dissociated phosphate anion. The hydration species of ethylmercuric ion would be expected to be pH dependent. Application of two-dimensional indirect detection shows that both the $^{199}$Hg chemical shift and line width of ethylmercury vary as a function of pH (Figure 4). This pH dependence reflects in fast exchange:

$$\underset{\text{I}}{2CH_3CH_2Hg^+} \overset{^-OH}{\rightleftharpoons} \underset{\text{II}}{(CH_3CH_2Hg)_2OH^+} \overset{^-OH}{\rightleftharpoons} \underset{\text{III}}{2CH_3CH_2HgOH}$$

The chemical shift range for these ethylmercury species is 120 ppm. The mercury line width is about 15 Hz at pH 3; it increases to 35 Hz at pH 4 and becomes even broader (>130 Hz) as the pH increases and $CH_3CH_2HgOH$ is produced. This behavior may indicate that the hydroxide is colloidal in nature.

**Ethylmercury–Amino Acid Adducts.** If 1:1 complexes of ethylmercury phosphate and free amino acids or other ligands are examined, a much larger range of chemical shifts is seen (about 600 ppm). The data are summarized in Table I. Within this large range three distinct clusters of mercury chemical shifts can be discerned. The sulfhydryl ligands cluster around 520 ppm. "Free" ethylmercury, or rather, the oxygen-chelated species, shows mercury chemical shifts at 0 ppm (referenced to EMP at pH 7.0). A large collection of amino acid adducts cluster at a point between these two extremes at about 200 ppm. These are attributed to ethylmercury–nitrogen complexes. Within the group of mercury–nitrogen adducts, there is a further dependence of chemical shift on the type of Hg–N adduct. At 220–200 ppm one finds adducts with the $\alpha$-$NH_2$ of aromatic and nonpolar amino acids. Ethylmercury adducts with the $\alpha$-$NH_2$ of acidic amino acids (aspartate, glutamate) are found around 197 ppm; the corresponding amides have slightly deshielded chemical shifts (186 ppm).

For several of the ethylmercury adducts there is evidence of slow chemical exchange between different species. This is detected as two major perturbations (inversions or nulls) when one steps through the mercury frequencies in the heteronuclear spin-echo experiment. Generally, one perturbation appears at the frequency of the "free" ethylmercuric ion (~0 ppm) and the other at a nitrogen (~200 ppm) or sulfur (~500 ppm) binding resonance. In most cases, one observes a null or a satellite inversion at the $^{199}$Hg frequency of the preferential binding site and a null or a slight decrease in satellite amplitude for the less populated site. This behavior reflects slow exchange between "free" ethylmercury

Table I. $^{199}$Hg Chemical Shifts of Amino Acid (or Analogue) and *N*-Acetyl Amino Acid Adducts with Ethylmercury[a]

| | free amino acid | | *N*-acetyl amino acid | |
|---|---|---|---|---|
| ligand | pH | $\delta_{Hg}$[b] | pH | $\delta_{Hg}$ |
| Ala | 7.0 | 197 (±12)[c] | | |
| Arg | 9.5 | 176 (±12) | 7.0 | −10 (±12) |
| Asn | 7.1 | 186 (±12) | 7.5 | 21 (±12) |
| Asp | 2.6 | −41 (±12) | | |
| | 7.0 | 197 (±12) | 7.0 | −10 (±12) |
| Cys | 1.6 | 528 (±12) | | |
| | 6.0 | 552 (±1) | 9.8 | 543 (±1) |
| $(Cys)_2$ | 7.0 | 248 (±12) | | |
| Glu | 7.0 | 197 (±12) | 2.2 | −41 (±2) |
| Gln | 7.0 | 186 (±12) | | |
| Gly | 3.8 | 7 (±12) | | |
| | 7.5 | 193 (±1) | 7.0 | 0 (±12) |
| His | 7.0 | 153 (±2) | 3.2 | 135 (±12) |
| | | | 7.0 | 135 (±12) |
| Ile | 7.0 | 197 (±12) | | |
| imidazole | 8.0 | 134 (±8) | | |
| Leu | 7.0 | 217 (±12) | | |
| Lys (1:1) | 9.4 | 176 (±12)[d] | 5.0 | −31 (±12)[f] |
| (2:1) | | 124 (±12)[e] | 8.5 | 176 (±12)[f] |
| | | | 3.0 | −28 (±12)[g] |
| | | | 7.0 | 135 (±12)[g] |
| β-mercapto-ethanol | 7.3 | 528 (±40) | | |
| Met | 7.4 | 217 (±12) | 7.0 | 10 (±12) |
| Phe | 7.1 | 217 (±12) | | |
| Pro | 7.0 | −10 (±12) | | |
| Ser | 7.0 | 186 (±12) | 7.0 | 0 (±12) |
| Thr | 7.2 | 197 (±12) | | |
| Trp | 3.1 | 217 (±12) | | |
| Tyr | | | 7.0 | −10 (±12) |
| Val | 7.1 | 197 (±12) | | |

[a] Samples are 40 mM amino acid/40 mM ethylmercury phosphate; the mercury chemical shift (ppm) is referenced to "free" ethylmercury at pH 7.0. Chemical shifts were determined primarily by spin-echo detection. [b] For all ethylmercury complexes except those with Arg, Cys, His, and Lys, two mercury resonances are detected by a decrease or null in the satellite amplitude upon mercury irradiation. One resonance corresponds to "free" ethylmercuric ion, the other is a N or S adduct. The mercury chemical shift listed belongs to the dominant (i.e., more inverted) species. [c] Errors in $^{199}$Hg chemical shifts are shown in parentheses. [d] Ethylmercury/Lys = 1:1. [e] Ethylmercury/Lys = 2:1; both lysine amino groups can interact with $^{199}$Hg. [f] $N^{\epsilon}$-Acetyllysine; ethylmercury adduct with the α-amino group. [g] $N^{\alpha}$-Acetyllysine; ethylmercury adduct with the ε-amino group.

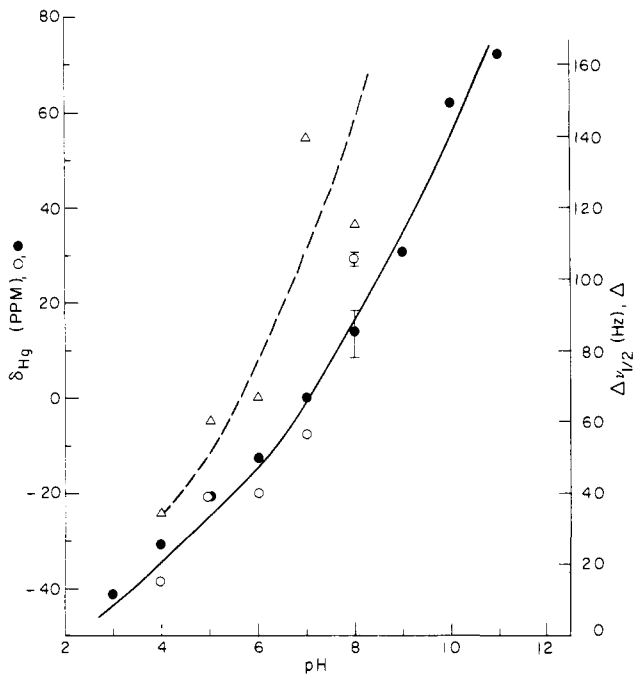


**Figure 4.** The pH dependence of the EMP $^{199}$Hg line width (△) and chemical shift (○) determined by two-dimensional (spin-echo) indirect detection; the comparable $^{199}$Hg chemical shifts (●) determined by spin-echo detection method are also shown.

and amino acid bound ethylmercury. Given the large chemical shift difference in hydrated ethylmercury and N adducts, one can estimate the mean residence lifetime as $\tau >> 1/\Delta\omega = 16\ \mu s$. Since in the $^1$H NMR regime species are in fast exchange (only one $^3J_{HgCH_3}$ average multiplet is observed), an upper estimate of $\tau$ is 3 ms. This slow exchange on the $^{199}$Hg NMR time scale allows us to estimate the population of the different species, and hence an apparent $K_D$ = [free amino acid][ethylmercury]/[ethylmercury–amino acid]. The decrease in the amplitude of the mercury satellite resonance is directly proportional to the amount of ethylmercury species at that particular mercury resonance frequency. If the decrease in satellite amplitude is summed for all ethylmercury species in slow exchange, a complete inversion corresponding to 100% of the satellite should be observed and a qualitative value for $K_D$ may be obtained. For example, for ethylmercury complexes with the $\alpha$-$NH_2$ of isoleucine and valine at pH 7, the methyl satellite nulls upon mercury irradiation at −10 ppm and 197 ppm, indicating roughly a 50:50 distribution of ethylmercury in free and N-bound forms. An estimate of $K_D$ is therefore 20 mM.

Intermediate exchange between two different N–Hg species (where the chemical shift difference is not as large) is detected by large line widths in the two-dimensional mercury spectrum. In the case of free histidine both the $\alpha$-amino and ring nitrogens can compete for binding the organomercurial. The mercury line width for ethylmercury–histidine is 364 Hz compared to 50 Hz observed for ethylmercury–imidazole, where only one of these sites is available.[6] *N*-Acetyl blocked amino acids were examined for complex formation with EMP to confirm that many of the mercury chemical shifts for ethylmercury adducts with amino acids reflect $\alpha$-amino–ethylmercury binding. The results are shown in Table I. With the exception of $N^{\alpha}$-acetyllysine, $N^{\epsilon}$-acetyllysine, *N*-acetylhistidine, and *N*-acetylcysteine, the $^{199}$Hg chemical shifts of the N-blocked amino acids are all equivalent to "free" ethylmercury at pH 7. The series of lysine adducts are particularly interesting. Both the $\alpha$- and $\epsilon$-amino groups can serve as ligands for ethylmercury. Their chemical shifts are quite distinctive: $\alpha$-amino adduct, 176 ppm; $\epsilon$-amino adduct, 135 ppm. In a 1:1 complex of free lysine with ethylmercury, the $\alpha$-amino group preferentially acts as the ligand. This probably reflects the $pK_a$ difference of the two amino groups. Lysine chelation of ethylmercury is pH dependent. At pH ≤5, only free ethylmercuric ion is observed. In fact, all the $\alpha$-amino–ethylmercury complexes are labile to acid pH (for example in Table I, aspartate and glycine at pH less than 4). Only complexes of ethylmercury with histidine, tryptophan, and cysteine are intact at acid pH values.

Ethylmercury complexes with other small molecules show $^{199}$Hg chemical shifts that reflect the Hg–X interaction. For example, with 2-mercaptoethanol, the ethylmercury resonance is at 528 (±40) ppm, very nearly that of cysteine. The ethylmercury imidazole $^{199}$Hg chemical shift is equivalent to that of histidine.

**PHMB Adducts with Amino Acids.** The interactions of an aromatic organomercurial, *p*-(hydroxymercuri)benzoate (pHMB), with different amino acids were also examined by $^{199}$Hg NMR. For this compound, satellites of the aromatic ring protons were examined with the spin-echo techniqu ($^3J_{HHg}$ = 182 Hz for the free organomercurial; 164 Hz for cysteine complex). *p*-(Hydroxymercuri)benzoate and mixtures with amino acids other than cysteine are only soluble at reasonable concentrations at pH 11. They exhibit $^{199}$Hg chemical shifts comparable to free ethylmercury (−4 ± 2 ppm). In contrast, the pHMB–cysteine complex is soluble at pH 7; the $^{199}$Hg chemical shift is 401 (±13) ppm. This aromatic organomercurial is much more selective in its reactions than the ethylmercuric ion. The $^{199}$Hg chemical shift difference between the free aromatic compound and its S–Hg adduct is about two-thirds that of the ethylmercury compounds.

**Ribonuclease Modification by Ethylmercury Phosphate.** Ribonuclease, which has been thoroughly studied by $^1$H NMR[16] spectroscopy and subjected to a wide variety of chemical modifications,[17] is a good protein with which to evaluate the usefulness of $^{199}$Hg NMR spectroscopy in identifying organomercurial complexes. It forms a 1:1 complex with ethylmercury; the activity of this complex is 75% that of the unmodified ribonuclease. Since this enzyme has no free sulfhydryl groups, the likely candidates for the site of ethylmercury modification include histidine, tryptophan, $\epsilon$-amino group of lysine, and the N-terminal amino group. All these ethylmercury–nitrogen bonds are unstable to amino acid hydrolysis. A comparison of the $^1$H NMR spectra of ribonuclease and ethylmercury–ribonuclease is not very enlightening. Addition of ethylmercury phosphate to ribonuclease causes protein aggregation, which is detected by increased line widths in the ribonuclease proton spectrum (Figure 5A). Because of this, a difference spectrum of unmodified and ethylmercury ribonuclease is of little help in identifying the ethylmercury ligand.

The relatively low concentration of ribonuclease (4 mM in protein, <1 mM in $^{199}$Hg) requires indirect detection of the mercury resonance by a difference spin-echo technique. This involves subtracting a proton spectrum of the ethylmercury–protein complex obtained without $^{199}$Hg irradiation from a spectrum acquired with on-resonance mercury irradiation. At the mercury resonance frequency, (which is determined ±12 ppm) the methylmercury satellite will add to give a negative peak while all the protein resonances will be nulled. At pH 7, difference spectra for irradiation at mercury frequencies corresponding to free ethylmercury, sulfhydryl, or $\alpha$-amino adducts are null (Figure 5C). A difference spectrum showing the $^{199}$Hg-coupled methyl satellites is only observed for irradiation corresponding to a mercury chemical shift of 135 ppm (Figure 5B). The methyl satellites appear centered in the $^1$H NMR spectrum at 1.09 ppm ($^3J_{HHg}$ = 300 Hz). Such a mercury frequency most likely belongs either to a histidine residue or to a lysine amino group (Table I). Discrimination between these two possibilities is provided by obtaining mercury spin-echo difference spectra at pH 3. Ethylmercury–lysine complexes are unstable at acid pH (Table I). If ethylmercury modifies a lysine in ribonuclease at pH 7, lowering the pH to 3 should release the ethylmercury. The mercury resonance frequency will now be that of the free ethylmercuric ion; irradiation at 135 ppm will produce a null

(16) Several key $^1$H NMR studies of ribonuclease are as follows: (a) Meadows, D. H.; Markley, J. L.; Cohen, J. S.; Jardetzky, O. *Proc. Natl. Acad. Sci. U.S.A.* **1968**, *58*, 1307. (b) Markley, J. L. *Biochemistry* **1975**, *14*, 3546. (c) Benz, F. W.; Roberts, G. K. C. *J. Mol. Biol.* **1975**, *91*, 345.

(17) Richards, F. M.; Wyckoff, H. W. *Enzymes, 3rd Ed.* **1971**, *4*, 647–806.

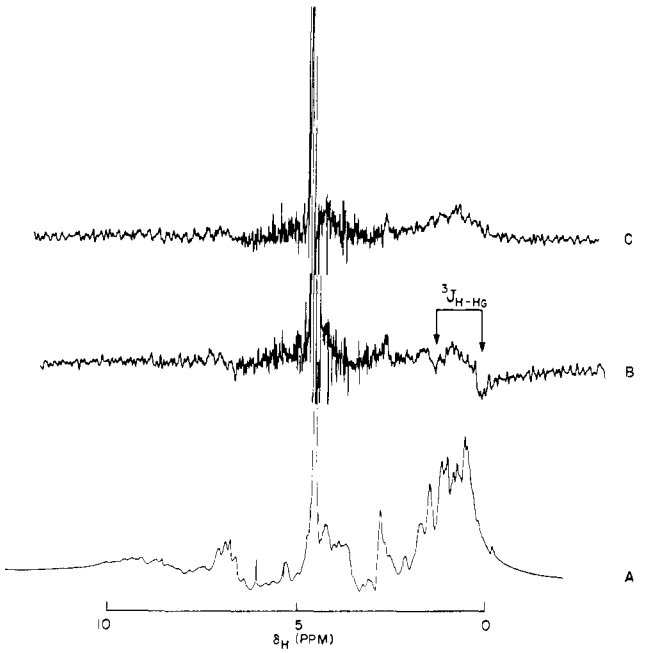


**Figure 5.** Ethylmercury phosphate modification of ribonuclease: (A) Proton spectrum of the ethylmercury–ribonuclease complex (pH 7) with mercury-199 irradiation off-resonance. (B) Proton difference spectra of the complex with $^{199}$Hg irradiation on-resonance at 135 ppm (satellite inversions occur centered at 1.09 ppm with $^3J_{HHg}$ = 300 Hz). (C) Proton difference spectrum of the ethylmercury–ribonuclease complex with $^{199}$Hg irradiation off-resonance.

difference spectrum. If the complex is with histidine, the $^{199}$Hg chemical shift should be largely unaltered. Experimentally, for ethylmercury ribonuclease at pH 3, $^{199}$Hg irradiation at 135 ppm results in a null difference spectrum (analogous to Figure 5C). $^{199}$Hg irradiation at 0 ppm yields a difference spectrum with inverted methyl satellites centered at 1.09 ppm with a $^3J_{HHg}$ = 340 Hz (a value consistent with free ethylmercuric ion). This strongly suggests that ethylmercury phosphate modifies a lysine amino group in ribonuclease.

The modification of a lysine in ribonuclease is particularly interesting in light of previous modification studies. There are 11 amino groups in ribonuclease A: the $\alpha$-amino group of lysine-1 and 10 lysine $\epsilon$-amino groups. Lysine-41 is located at the active site in ribonuclease and has an unusually low p$K_a$. It is about 70 times as reactive as the $\alpha$-amino of a dipeptide (or the N terminus) with modification reagents. However, modification of this lysine causes substantial loss of enzyme activity. Inorganic phosphate, which is a competitive inhibitor of ribonuclease, blocks lysine-41 from modification (it also protects histidine-119 and -12). Since phosphate is the ethylmercuric counterion, under our modification conditions the active site should be protected from the organomercurial. A lysine residue other than 41 (or 7, whose reactivity depends on prior reaction of 41) must be the site of the ethylmercury complex. It has been shown previously that modification of the ribonuclease N-terminal lysine barely affects enzyme activity (60% residual activity).[17] Because our ethylmercury adduct is 75% as active as unmodified ribonuclease, we suggest that lysine-1 is the site of modification. While the mercury chemical shift is more in accord with an $\epsilon$-amino group rather than an $\alpha$-amino group, the magnitude of this shift difference (40 ppm) could reflect environmental effects on the protein-bound ethylmercury moiety. For comparison, the chemical shift range for ethylmercury–$\alpha$-amino complexes with a large series of amino acids is 41 ppm (176–217 ppm).

## Summary

$^{199}$Hg NMR spectroscopy by indirect detection is potentially useful in analyzing organomercury interactions with biomolecules. The large chemical shift range allows easy identification of the heteroatom (O, N, S) bound to the mercury. Furthermore, the large differences in chemical shifts guarantee that organomercury in these classes will be in slow exchange. This property should make it a good technique for identifying ligands in complex mixtures with organomercurials.

**Acknowledgment.** We are indebted to Dr. David J. Ruben for valuable assistance with the instrumentation. The high-field NMR experiments were performed at the NMR facility for Biomolecular Research located at the F. Bitter National Magnet Laboratory, M.I.T. The NMR facility is supported by grant RR00995 from the Division of Research Resources of the National Institutes of Health and by the National Science Foundation under Contract C-670. Support from the National Institutes of Health, GM 26762 to M.F.R., is also gratefully acknowledged.

**Registry No.** Ala ethylmercury adduct, 82798-56-9; Arg ethylmercury adduct, 82798-57-0; Asn ethylmercury adduct, 82798-59-2; Asp ethylmercury adduct, 82798-61-6; Cys ethylmercury adduct, 82798-63-8; $(Cys)_2$ ethylmercury adduct, 82798-65-0; Glu ethylmercury adduct, 82798-66-1; Gln ethylmercury adduct, 82798-68-3; Gly ethylmercury adduct, 82798-69-4; His ethylmercury adduct, 82798-71-8; Ile ethylmercury adduct, 82798-72-9; Leu ethylmercury adduct, 82798-73-2; Lys ethylmercury adduct (1:1), 82798-74-1; Lys ethylmercury adduct (2:1), 82798-75-2; Met ethylmercury adduct, 82798-79-6; Phe ethylmercury adduct, 82798-81-0; Pro ethylmercury adduct, 82798-82-1; Ser ethylmercury adduct, 82798-83-2; Thr ethylmercury adduct, 82798-85-4; Trp ethylmercury adduct, 82798-86-5; Val ethylmercury adduct, 82798-88-7; *N*-acetyl-Arg ethylmercury adduct, 82798-58-1; *N*-acetyl-Asn ethylmercury adduct, 82798-60-5; *N*-acetyl-Asp ethylmercury adduct, 82798-62-7; *N*-acetyl-Cys ethylmercury adduct, 82798-64-9; *N*-acetyl-Glu ethylmercury adduct, 82798-67-2; *N*-acetyl-Gly ethylmercury adduct, 82798-70-7; *N*-acetyl-His ethylmercury adduct, 82798-90-1; *N*-$\epsilon$-acetyl-lys ethylmercury adduct, 82798-76-3; *N*-$\alpha$-acetyl-Lys ethylmercury adduct, 82798-77-4; *N*-acetyl-Met ethylmercury adduct, 82798-80-9; *N*-acetyl-Ser ethylmercury adduct, 82798-84-3; *N*-acetyl-Tyr ethylmercury adduct, 82798-87-6; imiadazole ethylmercury adduct, 82798-91-2; 2-mercaptoethanol ethylmercury adduct, 82798-78-5; pHMB, 1126-48-3; $^{199}$Hg, 14191-87-8; pHMB–cysteine complex, 82798-89-8; ethylmercury ion, 21687-36-5; ethylmercury phosphate, 2235-25-8; ribonuclease, 9001-99-4; lysine, 56-87-1.